Quantification of fluorescence in thick specimens, with an application to cyclin B–GFP expression in starfish oocytes

Mark Terasaki[1]

Department of Cell Biology, University of Connecticut Health Center, 263 Farmington Ave, Farmington, CT 06032, U.S.A.

Background information. Fluorescence imaging of living cells is widely used in cell biology. It is now being extended to thick specimens such as large cells or tissues where it is important to establish methods for obtaining quantitative fluorescence data due to the increasing importance of computational and systems biology approaches.

Results. Fluorescent solutions were used as a calibration standard for determining cellular fluorescence concentrations from z series image sequences. The accuracy of the measurements was evaluated using quantitatively injected cells. Different fluorescence attenuation rates of the cytoplasm and nucleoplasm were documented, and autofluorescence levels were determined. This method was used to characterize the effect of cyclin B overexpression on cell-cycle timing in starfish oocytes. The time interval between application of maturation hormone and germinal vesicle breakdown decreased with increasing cyclin B–GFP (green fluorescent protein) concentration to a level of 100–300 nM, beyond which there was no effect.

Conclusions. Conditions for determining fluorescent probe concentrations in large cells or multicellular tissues were established, which will facilitate the collection of data for quantitative studies. This method was used to characterize the effect of cyclin B–GFP expression levels on cell-cycle timing in starfish oocytes.

Introduction

It is of increasing interest to measure the concentration of a fluorescent probe within a cell or tissue. Systematic approaches have been worked out for variants of this problem, mostly the quantification of fluorescent objects that are small relative to the z resolution limit of the microscope. In one study, a detailed analysis was made for relatively thin (<10 μm thick) N1E-115 neuroblastoma cells in culture (Fink et al., 1998). A three-dimensional computer model of various cell geometries and subcellular structures was blurred with the point spread function of a confocal microscope to show how the structure would look in the microscope, then subjected to a restoration algorithm to show how to derive the actual concentrations and distributions from the microscope image. In another study, solutions of GFP (green fluorescent protein) were used as a standard towards the quantification of GFP-tagged proteins within organelles of the secretory system of thin, cultured cells (Hirschberg et al., 1998). Values for the thickness of the confocal optical section were used to calculate the number of GFP molecules corresponding to a fluorescence signal; this approach was tested by imaging drops of GFP solution that have a smaller diameter than the optical section. A third study was concerned with quantifying fluorescently labelled acetylcholine receptors in living animals (Turney et al., 1996). In this work, it was desired to monitor turnover of neuromuscular junction receptors over a period of days or months. A standard material, spectralon, was adopted as a fluorescent standard and was used to correct for day-to-day variations in light source brightness, microscope and camera performance and background autofluorescence.
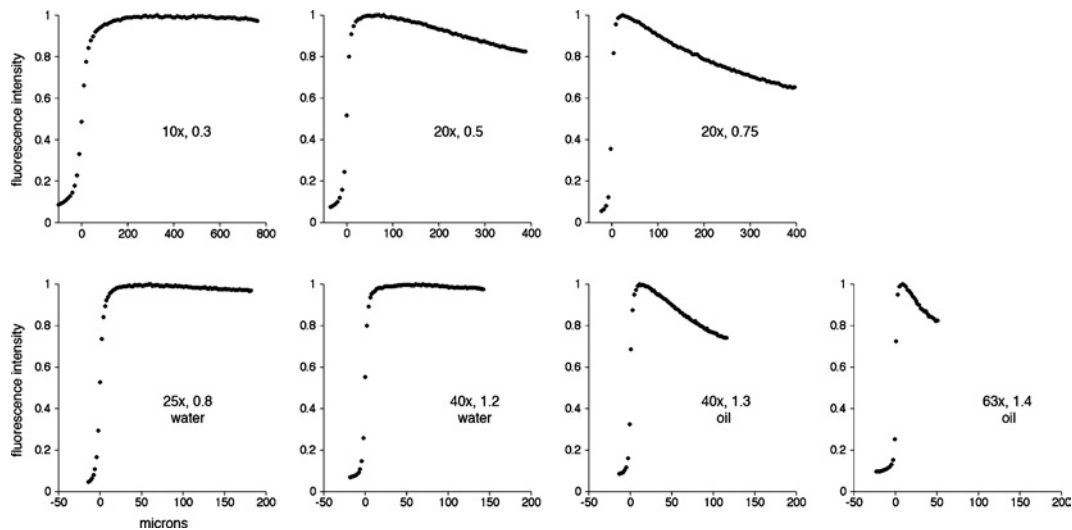
Figure 1 | z series of a fluorescent solution (1.6 μM 10 kDa rhodamine–dextran in a 3.25 mm thick chamber) using different objective lenses

The confocal aperture setting was at 5 (fully open = 15). The position of the focal plane along the z direction is plotted on the x-axis, as in most of the other Figures. Note the different scales on the x-axis for the top and bottom rows.

An approach for quantifying fluorescence in thick specimens is described in the present paper, along with an application to the effect of cyclin B–GFP overexpression on cell-cycle timing.

Results and discussion
z series of fluorescent solutions
A solution of fluorescent molecules is a uniform specimen, and a microscope system intended for characterizing fluorescence in thick specimens should ideally give a z series with a uniform signal. A 1 mm thick chamber of an aq. 1.6 μM solution of rhodamine-conjugated 10 kDa dextran was imaged with several different objective lenses (Figure 1). With a ×10, 0.3 NA (numerical aperture) lens, the signal remained constant for at least 500 μm. With both a ×25, 0.8 NA water immersion lens and a ×40, 1.2 NA water immersion lens, the z series was also constant, to the depth permitted by their shorter working distance (Figure 1). However, with some other lenses, the fluorescent signal decreased significantly. The fluorescence signal with a ×20, 0.5 NA lens decreased slowly, so that there was a small but significant decrease by approx. 100 μm, whereas, with a ×20, 0.75 NA lens, there was a higher rate of decrease (Figure 1). The z series signal obtained with the
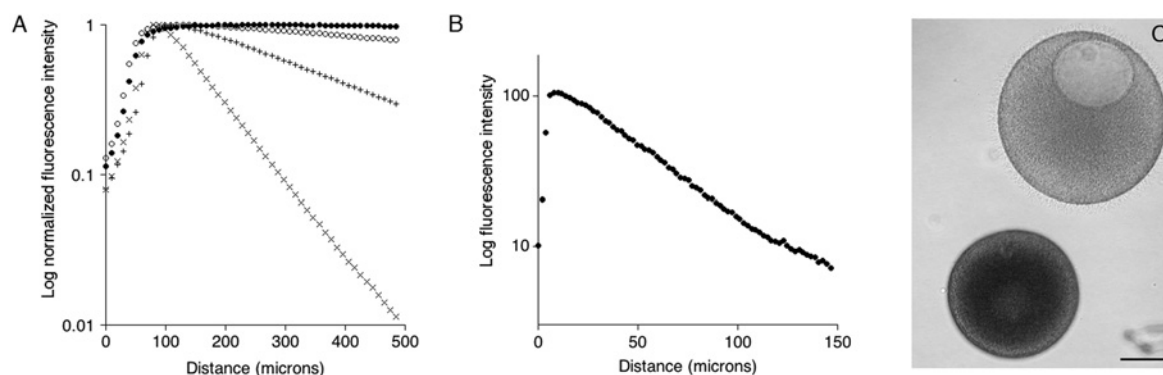
oil immersion ×40, 1.3 NA or ×63, 1.4 NA lenses decreased even more rapidly (Figure 1).

The non-ideal decreases in fluorescence with depth are due to spherical aberration of the objective lenses, in which light that passes through the peripheral edge of the lens focuses on to a different position on the z-axis than light that passes through the centre of the lens. As a result of this aberration, fluorescence is excited in a greater volume than ideal. The problem is compounded because the emitted light is subject to the same aberration on the return path: fluorescence is emitted in all directions and is collected by the objective lens, but the emission light that passes through the centre versus the periphery is not focused at the same position on the z-axis. Water immersion lenses can be corrected for spherical aberration at different depths because the light passes through only water and a defined amount of glass (the thickness of the coverslip). For oil immersion and air lenses, the light travels through variable amounts of oil/air and water as the focus depth changes, making it difficult or impossible to correct this problem for all focus depths with one lens design.

The z series of a solution can also be non-constant due to high fluorescence concentrations. At higher concentrations, a significant fraction of the excitation light is absorbed in the superficial layers of

Figure 2 | Attenuation of fluorescence in solutions and in cytoplasm

(**A**) Signal decrease due to increasing concentrations of a fluorescent molecule as described by the Beer's Law. Four calcein solutions were imaged with a ×10, 0.3 NA lens: 8 μM (●), 40 μM (○), 200 μM (+) and 800 μM (×). The fluorescence decreased exponentially as shown in the logarithmic plot. The data correspond to molar absorption coefficients of 79 000, 75 000, and 63 000 $M^{-1} \cdot cm^{-1}$ for 40, 200 and 800 μM calcein respectively, while the molar absorption coefficient for fluorescein (the parent compound of calcein) was 67 000 $M^{-1} \cdot cm^{-1}$ (Tsien and Waggoner, 1995). (**B**) Attenuation of fluorescence by the cytoplasm. A starfish oocyte was injected with 10 kDa rhodamine–dextran (final concentration 8 μM) and then imaged with a ×40, 1.2 NA objective lens. As shown in the logarithmic plot, the fluorescence decrease is fit well by an exponential decay, with a distance for half-attenuation of 32 μm. (**C**) Transmitted light image of a fully grown oocyte (upper right) and a growing oocyte (lower left). The cytoplasm of the growing oocyte is less transparent, and there is a correspondingly greater attenuation of cytoplasmic fluorescence in a z series (distance for half-attenuation was 16 μm). Scale bar, 50 μm.

Table 1 | Approximate values for the optical section of selected objective lenses

The Table shows the distance between the 10 and 90% intensity values of a z series in the region of the coverglass/fluorescent solution interface. Values were determined for three settings of the confocal aperture (15 is the maximum opening on this microscope).

Confocal aperture	Optical section (μm)				
	×10, 0.3 NA	×20, 0.5 NA	×20, 0.75 NA	×40, 1.3 NA	×63, 1.4 NA
5	95	23	16	7.5	4.3
10	110	34	23	9	5.5
15	175	47	30	13	6.5

fluorescent dye solution, resulting in less excitation light at deeper levels (equivalently, the photons are being depleted from the excitation light). The effect of this depletion of excitation light is described by Beer's Law (see the Materials and methods section). A z series of increasing concentrations of calcein with the ×10, 0.3 NA lens shows decreases that are fit by an exponential decline as predicted by Beer's Law (Figure 2A). For many cell experiments, the thickness of the cells and the concentration of the fluorescent molecules are small enough that Beer's Law does not need to be considered.

The optical sectioning properties of the lens and confocal pinhole affect the transition in the z series between outside and inside the solution. At higher NAs and at smaller pinhole settings, the increase becomes steeper. The distance between 10% and 90% brightness gives an approximate value for the depth from which the fluorescence is collected (Table 1).

z series of the cytoplasm

Immature starfish oocytes are 170–180 μm in diameter. An oocyte was injected with 10 kDa rhodamine–dextran (final concentration 16 μM), then imaged with a ×40, 1.2 NA water immersion lens. With this lens and concentration, a z series of a fluorescent solution is constant, but the z series of cytoplasmic fluorescence decreased (Figure 2B). The fluorescence is fit by an exponential decrease, and can be explained by absorption or scattering of a constant fraction of light per unit thickness of cytoplasm.

One obstacle to quantification is biological variation. There seems to be a significant variation in the rate of fluorescence decrease depending on the batch of oocytes. For instance, the characteristic distance at which fluorescence decreases to half was 29.8 ± 2.1 μm (S.D., $n = 5$) for oocytes from one animal, but was 36.5 ± 3.4 ($n = 5$) for oocytes from another animal.

Different cell types have different degrees of opacity. There are sometimes small oocytes in the preparation of starfish oocytes and they appear more dense than the fully grown immature oocytes used for these experiments (Figure 2C). Correspondingly, the distance in which fluorescence decreases to half in these small oocytes was much shorter (16.0 ± 2.0 μm; $n = 4$).
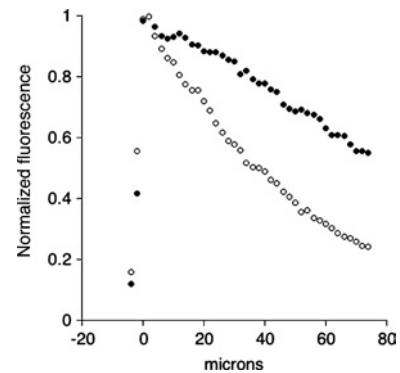
Eggs and embryos of the hemichordate *Saccoglossus kowalevskii* are so opaque that the nucleus cannot be seen by transmitted light microscopy (Lowe et al., 2004). Consistent with this, the intracellular fluorescence decreases with a half-length of 5.8 ± 0.5 μm ($n = 5$). Mouse oocytes, on the other hand, are more clear; their intracellular fluorescence decreases with a half-length of 42.8 ± 8.8 ($n = 3$).

Attenuation with depth by multiphoton microscopy was also characterized. Using the same microscope and the same rhodamine–dextran-injected oocytes, z series sequences were obtained in three different ways: by conventional confocal microscopy with 543 nm laser excitation, or by using multiphoton excitation by 800 nm light from a Ti-Sapphire laser in either descan or non-descan mode (Figure 3). Using confocal microscopy, the half-distance for attenuation was 35.6 ± 2.3 μm ($n = 7$). In the multiphoton de-scan mode, where the emission light travels the same path as in confocal microscopy, the half-distance for attenuation was 42.6 ± 2.4 μm ($n = 7$). The slightly longer distance may be consistent with the greater penetrating ability of the longer-wavelength excitation light. For the non-descan mode, where the emission light is collected before returning to the galvanometer mirrors, the half-distance was 82.9 ± 4.2 μm ($n = 7$).

Confocal microscopes are designed to collect non-scattered emitted light that originates at the focal plane of the objective; the optics focus this light at the confocal pinhole. As the depth increases and the scattering becomes greater, larger amounts of light are lost because the scattered light is not focused

Figure 3 | Attenuation of cytoplasmic fluorescence observed by confocal versus multiphoton microscopy
Oocytes were injected with 10 kDa rhodamine–dextran and imaged with the same microscope and lens by the two methods. Attenuation was less with multiphoton microscopy (non-descan mode; ●) than with confocal microscopy (○).

correctly. With multiphoton microscopy, the emitted light originates only at the focal plane due to the multiphoton excitation, so that the optics can be designed to collect as much of the emitted light as possible, including the scattered emitted light (Denk and Svoboda, 1997); this leads to the difference in attenuation.
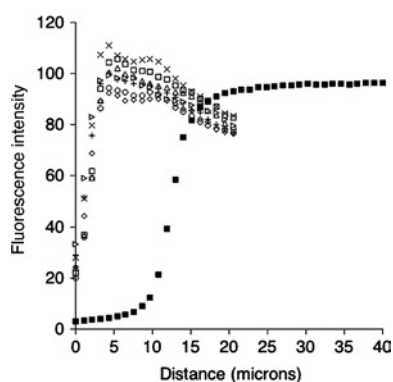
Quantification of cytoplasmic fluorescence

To test whether a fluorescent solution can be used as a calibration standard for cellular fluorescence, eggs were injected with a known amount of fluorescent dye and compared with a solution. Quantitative micro-injection methods for injecting echinoderm eggs were originally developed by Hiramoto (1962) and by Kiehart (1982).

A 1% volume injection of a stock solution of 1.6 mM 10 kDa rhodamine–dextran was made into seven oocytes. The z series signals from the oocytes varied by approx. 10%, which could be partially due to variability in oocyte volumes. When these signals were compared with that of a 1% dilution of the same stock solution in sea water, the maximum values were close to the plateau value of the solution z series (Figure 4). In this case, then, the maximum cell fluorescence corresponds closely to the plateau level of a fluorescence solution of the same concentration. This indicates that the unknown concentration of a fluorescent molecule in a cell can be estimated by comparing the maximum cell fluorescence in a z series with that of a fluorescent solution of known concentration.

Figure 4 | Comparison of the signal from the same concentration of fluorescent marker in the cytoplasm versus solution

A 1.6 mM 10 kDa rhodamine–dextran stock solution was diluted 1:100 in sea water and imaged as a 16 μM solution with a ×40, 1.2 NA objective lens. Starfish oocytes were quantitatively injected with a 1% volume injection of the same rhodamine–dextran stock solution to give a final cytoplasmic concentration of 16 μM, and were imaged with the same lens and microscope settings. The z series for each of the seven injected oocytes is shown in the graph. The constant level of the fluorescent solution corresponds well to the maximum of the cytoplasmic z series. For the data shown, the maximum fluorescence of injected oocytes was 100.7 ± 6.4 ($n = 7$) compared with the solution plateau value of 96. Injections were made on two other occasions with oocyte per solution measurements of 108.4 ± 7.7 ($n = 7$)/117 and 124.8 ± 5.6 ($n = 7$)/116. The solution intensity is subject to variability from pipetting; using a 1 μl volume to make a solution resulted in normalized plateau values of 100 ± 8.8 ($n = 6$).
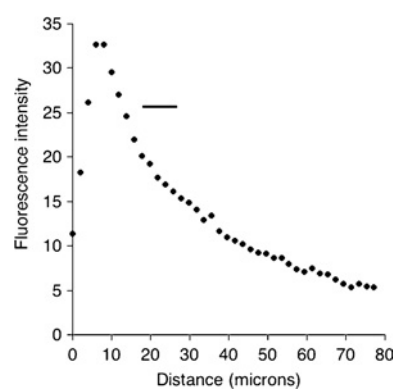

Autofluorescence

Oocyte autofluorescence was imaged with settings that gave approx. 40 times the sensitivity of the settings used in Figure 2(B) for injected fluorescence. There is a cortical layer of large (1 μm diameter) vesicles that have a significant autofluorescence signal at these microscope settings. These vesicles gave rise to a bump in the z series, so that it was necessary to estimate the maximum of the cytoplasmic autofluorescence by extrapolation of the signal from the deeper levels (Figure 5). Autofluorescence levels were determined for 488 and 568 nm excitation in the fluorescein and rhodamine channels. For 568 nm excitation, the autofluorescence was equivalent to 76 ± 5 nM rhodamine ($n = 4$). For 488 nm excitation, the autofluorescence was equivalent to either 42 ± 5 nM calcein ($n = 4$) or

Figure 5 | Characterization of autofluorescence

An uninjected oocyte was imaged with a ×40, 1.2 NA lens in the fluorescein channel using high-sensitivity settings and relatively high light intensity (gain = 900, aperture = 5, slow scan at ~3 μs/pixel with low signal enhance; 47 μW back focal plane of the objective). The fluorescence signal decreases exponentially except at the very beginning of the decline, where the increased signal is due to autofluorescent vesicles present in the cortex. The horizontal line segment indicates the estimated maximum value of the cytoplasmic autofluorescence. When calibrated against a standard solution, the autofluorescence signal was equivalent to approx. 40 nM calcein or approx. 120 nM GFP.

122 ± 15 nM GFP (calcein is 2.9 times as bright as GFP on a molar basis). There appears to be a significant variation in the fluorescence for oocytes obtained from different animals. From four different animals, the autofluorescence varied between a low value of 83 ± 7.8 nM GFP ($n = 5$) and 157 ± 9.5 nM GFP ($n = 4$).
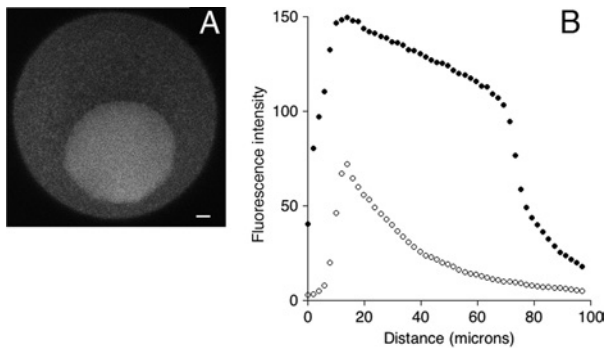
When a fluorescent probe of interest is present at a low concentration, the autofluorescence level must be subtracted from the observed signal. However, there is a cell-to-cell variation in the autofluorescence; for instance, in the fluorescein channel, this was equivalent to as much as 10 nM GFP. The subtraction of the autofluorescence level must include this variation; for measuring low concentrations, the variation in autofluorescence can be a more important limiting factor than the light sensitivity of the instrument.

The nucleus and the cytoplasm

The nucleus (germinal vesicle) of immature starfish oocytes is positioned near the cell surface at the animal pole. Small molecules pass freely between the cytoplasm and nucleus through nuclear pores. When

Figure 6 | Fluorescence of the cytoplasm versus the nucleus

(**A**) Rhodamine–dextran (10 kDa) was injected (16 µM final concentration) into oocyte cytoplasm and allowed to come to equilibrium between the cytoplasm and nucleus. Scale bar, 10 µm. (**B**) Fluorescence attenuation by the cytoplasm versus the nucleus. The nucleus of starfish oocytes is attached to the cortex at the animal pole. The oocyte was orientated so that the animal pole was close to the coverslip; this orientation minimizes the fluorescence attenuation due to intervening cytoplasm compared with other orientations. The oocyte was injected with calcein (final concentration 8 µM). A ×40, 1.2 NA lens was used to image the nuclear (●) and cytoplasmic (○) fluorescence. The nucleus/cytoplasm ratio varied from 2.1 at the shallowest level to 10.2 at the deepest level. The distance for half-attenuation in the nuclear interior was 230 ± 51 µm ($n = 3$).

a small fluorescent molecule is injected into the cytoplasm, it comes to an equilibrium in which the nucleus is more fluorescent than the cytoplasm (Figure 6A; 10 kDa rhodamine–dextran). This is due to different amounts of space that is available for diffusion. The nucleus is devoid of space-occupying organelles, while the cytoplasm contains many membrane-bound organelles, especially yolk platelets, which are 1–2 µm in diameter and occupy approximately half the cytoplasmic volume. Therefore the cytosolic concentration and nucleoplasmic concentration are very likely to be the same, whereas the cytoplasmic concentration is less than the nucleoplasmic concentration due to space exclusion by the yolk platelets.

In a z series, the fluorescence decreases more slowly in the nucleus than in the cytoplasm (Figure 6B). This is consistent with the transmitted light appearance, in which the nucleus appears clear and the cytoplasm appears mottled (e.g. Figure 2C). Due to the different decrease rates, the fluorescence bright-ness of the nucleus relative to the cytoplasm will depend on the focal plane; the nucleus will be relatively brighter at greater depths. In order to determine the actual nucleoplasmic/cytosolic ratio, oocytes were orientated with the animal pole close to the coverslip to minimize the effect of depth. Values for the nuclear and cytoplasmic fluorescence were taken at the maximum (see Figure 6B). By this measurement, the ratio of the cytoplasm and nucleus was found to be 2.07 ± 0.13 ($n = 5$).
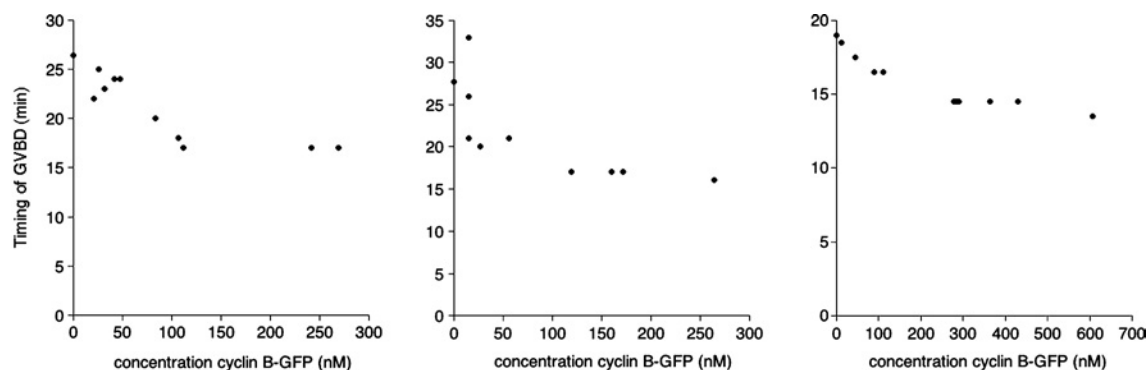
Cyclin B–GFP expression

Entry into M phase is regulated by the activity of Cdc2 (cell division control 2) kinase (Nurse, 1990). Cdc2 must be associated with cyclin B to be functional, and there is an excess of Cdc2 over cyclin B in cells. Cyclin B overexpression causes *Xenopus* oocytes to enter the M phase (Swenson et al., 1986) and synthesis of cyclin B is sufficient to drive a cell-free extract into M phase (Murray and Kirschner, 1989). Thus the amount of cyclin B can have direct effects on M phase entry, and its synthesis may govern the timing of early embryonic cell divisions.

A cyclin B–GFP chimaera is functional and allows localization of Cdc2–cyclin B in living cells (Hagting et al., 1998). We used cyclin B–GFP to image changes in localization of Cdc2–cyclin B during meiotic maturation of starfish oocytes (Terasaki et al., 2003). In these cells, the endogenous level of cyclin B is estimated to be 20 nM (E. Okumura and T. Kishimoto, personal communication). In order to image cyclin B–GFP adequately, we estimated that it was necessary to express it at several times the endogenous level. Cyclin B–GFP was expressed by injection of mRNA into immature oocytes, which were arrested at the G$_2$/M transition. Application of the maturation hormone relieves the arrest; cyclin B–GFP expression affected the cell cycle by shortening the time interval between application of maturation hormone and NEBD (nuclear envelope breakdown) (Terasaki et al., 2003).

The fluorescence measurement method described here was used to characterize this effect quantitatively. Different amounts of mRNA were injected into a number of oocytes, and after an overnight incubation period, the amount of cyclin B–GFP expressed in each oocyte was determined. Maturation hormone (1 µM 1-methyladenine) was then added to the oocytes, and the time interval to NEBD for each

Figure 7 | Effect of cyclin B–GFP expression level on cell-cycle timing

Different amounts of mRNA coding for cyclin B–GFP were injected and allowed to express overnight. The level of cyclin B–GFP present in each oocyte was determined using the z series approach established in the present paper. The maturation hormone 1-methyladenine was added to induce maturation. The oocytes were observed by transmitted light microscopy and the timing for NEBD was recorded for each oocyte. Results from three experiments are shown (different animals were used in each experiment). The graphs show the time of NEBD as a function of cyclin B–GFP expression. With increasing expression levels, the timing becomes shorter, but then reaches a plateau at approx. 100–300 nM.

oocyte was determined by light microscopy. The auto-fluorescence level (equivalent to 80–160 nM GFP) and its cell-to-cell variation (∼10 nM) made it difficult to measure cyclin B–GFP at concentrations lower than approx. 10–20 nM, which is approximately the endogenous concentration. At these concentrations, cyclin B caused the time interval to GVBD (germinal vesicle breakdown) to shorten significantly; increasing cyclin B–GFP concentrations shortened the interval further, but there was little effect beyond approx. 100 nM in oocytes from two animals and beyond approx. 200–300 nM in oocytes from a third animal (Figure 7). A simple explanation of these results is that cyclin B–GFP binds to free Cdc2 and speeds up the timing of GVBD until there is no longer any available free Cdc2.

The approach described here should be useful in quantitative studies involving large cells such as oocytes. These cells have many experimental advantages, such as the ability to be quantitatively injected, or the availability of a uniform population at the same cell-cycle stage. The quantification method should also be useful for fluorescence imaging of multicellular structures or tissues.

Materials and methods

Oocytes

Starfish (*Asterina miniata*) oocytes were obtained as described previously (Terasaki et al., 2003). Eggs from the hemichordate *S. kowalevskii* were obtained as described by Lowe et al. (2004).

A 2% injection of 800 μM calcein was made in the first 3 min after fertilization and observations were made with a ×40, 1.2 NA water immersion lens during the first cell cycle. Fully grown immature mouse oocytes were obtained as described by Kalinowski et al. (2004), allowed to mature spontaneously, injected with a 2% volume injection of 800 μM calcein, and imaged at room temperature (22–24°C).

Microscopy

An MRC 600 confocal microscope (Bio-Rad, Cambridge, MA, U.S.A.) with a krypton/argon laser was used. It was coupled with an upright Axioskop microscope (Carl Zeiss, Thornwood, NY, U.S.A.). All objective lenses used were obtained from Zeiss. Coverslips of 1.5 thickness were used for all observations. Measurements of light intensity were made with a laser power meter (Newport model 1815-C; Newport, Irvine, CA, U.S.A.). The transmitted light image in Figure 2(C) was taken with a digital camera (Epson 3100Z; Epson, Long Beach, CA, U.S.A.) positioned at the eyepiece of the microscope.

A Zeiss 510 NLO microscope with non-descan detection was used for multiphoton imaging. Rhodamine–dextran was excited by either a 543 nm He/Ne laser or a Mira Ti Sapphire laser pumped with an 8 W Verdi laser (Coherent, Santa Clara, CA, U.S.A.).

Solutions

Calcein and 10 kDa tetramethylrhodamine–dextran were obtained from Molecular Probes (Eugene, OR, U.S.A.). Calcein was made in a stock solution of 0.5 mg/ml (800 μM) in 100 mM potassium glutamate and 10 mM Hepes (pH 7). Rhodamine–dextran (10 kDa) was prepared as a stock solution of 10 mg/ml (800 μM rhodamine) in the same buffer. To make solutions for imaging, a micropipettor (Gilson, Middleton, WI, U.S.A.) was used to dilute 1 μl of solution in 100–1000 μl of sea water. A larger volume of working solution can be stored in a 50 ml polypropylene centrifuge tube; it should not be stored in a glass

scintillation vial because the fluorescence becomes dimmer by >50% over a period of several days, probably due to dye binding to the glass. The microscope chamber was made of 0.125 inch (3.175 mm) thick silicon rubber (calendared sheet; North American Reiss, Blacksburg, VA, U.S.A.) in which a small rectangular hole was cut with a razor blade. The chamber was sealed with silicone grease to a microscope slide, filled with approx. 100 µl of solution and then sealed with a coverslip.

Beer's Law ($A = \varepsilon c l$) relates light absorption to the distance of the light path, where A is the absorbance $\log_{10}(T_o/T)$ (with T = transmittance), ε is the molar absorption coefficient, c is the concentration (measured in mol/l) and l is the path length (measured in cm). To calculate the molar absorption coefficient from the exponentially declining z series fluorescence of a solution of known concentration, the distance at which the fluorescence had decreased by one-half was determined (usually from 90 to 45% brightness). At this distance, $A = \log_{10}(2) = 0.3$.

Recombinant EGFP (enhanced GFP) was obtained from Clontech/BD Biosciences (Mountain View, CA, U.S.A.) and stored in aliquots at −70°C. EGFP has very similar fluorescence properties as the S65T mutant of GFP that was used in the cyclin B–GFP chimaera (Tsien, 1998). The stock solution was diluted to 1.9 µM in sea water and imaged in the microscope chamber described above.

Quantitative injection

Quantitative injections were made as described by Jaffe and Terasaki (2004) (see also http://egg.uchc.edu/panda/injection).

Diagnostics

The signal intensity from a fluorescent solution depends on the excitation light energy, the lens used, the photomultiplier gain and the confocal aperture. By controlling these parameters, the fluorescence from a solution can be used to monitor the microscope alignment or condition of the fluorescence filters.

References

Denk, W. and Svoboda, K. (1997) Photon upmanship: why multiphoton imaging is more than a gimmick. Neuron **18**, 351–357

Fink, C., Morgan, F. and Loew, L.M. (1998) Intracellular fluorescent probe concentrations by confocal microscopy. Biophys. J. **75**, 1648–1658

Hagting, A., Karlsson, C., Clute, P., Jackman, M. and Pines, J. (1998) MPF localization is controlled by nuclear export. EMBO J. **17**, 4127–4138

Hiramoto, Y. (1962) Microinjection of live spermatozoa into sea urchin eggs. Exp. Cell Res. **27**, 416–426

Hirschberg, K., Miller, C.M., Ellenberg, J., Presley, J.F., Siggia, E.D., Phair, R.D. and Lippincott-Schwartz, J. (1998) Kinetic analysis of secretory protein traffic and characterization of golgi to plasma membrane transport intermediates in living cells. J. Cell Biol. **143**, 1485–1503

Jaffe, L.A. and Terasaki, M. (2004) Quantitative microinjection of oocytes, eggs and embryos. Methods Cell Biol. **74**, 219–242

Kalinowski, R.R., Berlot, C.H., Jones, T.L.Z., Ross, L.F., Jaffe, L.A. and Mehlmann, L.M. (2004) Maintenance of meiotic prophase arrest in vertebrate oocytes by a G_s protein-mediated pathway. Dev. Biol. **267**, 1–13

Kiehart, D.P. (1982) Microinjection of echinoderm eggs: apparatus and procedures. Methods Cell Biol. **25B**, 13–31

Lowe, C.J., Tagawa, K., Humphreys, T., Kirschner, M. and Gerhart, J. (2004) Hemichordate embryos: procurement, culture, and basic methods. Methods Cell Biol. **74**, 171–194

Murray, A.W. and Kirschner, M.W. (1989) Cyclin synthesis drives the early embryonic cell cycle. Nature (London) **339**, 275–280

Nurse, P. (1990) Universal control mechanism regulating onset of M-phase. Nature (London) **344**, 503–508

Swenson, K.I., Farrell, K.M. and Ruderman, J.V. (1986) The clam embryo protein cyclin A induces entry into M phase and the resumption of meiosis in Xenopus oocytes. Cell (Cambridge, Mass.) **47**, 861–870

Terasaki, M., Okumura, E., Hinkle, B. and Kishimoto, T. (2003) Localization and dynamics of Cdc2-cyclin B during meiotic reinitiation in starfish oocytes. Mol. Biol. Cell **14**, 4685–4694

Tsien, R.Y. (1998) The green fluorescent protein. Annu. Rev. Biochem. **67**, 509–544

Tsien, R.Y. and Waggoner, A. (1995) Fluorophores for confocal microscopy. In Handbook of Biological Confocal Microscopy (Pawley, J.B., ed.), 2nd edn, pp. 267–279, Plenum Press, New York

Turney, S.G., Culican, S.M. and Lichtman, J.W. (1996) A quantitative fluorescence-imaging technique for studying acetylcholine receptor turnover at neuromuscular junctions in living animals. J. Neurosci. Methods **64**, 199–208